Semarak Journal of Thermal-Fluid Engineering

Journal homepage: https://semarakilmu.my/index.php/sjotfe/index
ISSN: 3030-6639

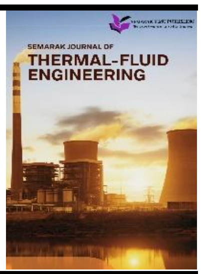

Analysis of Capillary Rise and Surface Tension in Micro-Tubes Using Computational Modelling

Chai Yu Pin[1], Ishkrizat Taib[1,*]

[1] Department of Mechanical Engineering, Faculty of Mechanical and Manufacturing Engineering, Universiti Tun Hussein Onn Malaysia, 86400 Parit Raja, Johor, Malaysia

ARTICLE INFO

Article history:
Received 26 April 2026
Received in revised form 5 May 2026
Accepted 22 May 2026
Available online 30 June 2026

ABSTRACT

Microfluidics technology is widely used in modern engineering, such as medical diagnostic chips and micro-electronic cooling devices. In small-scale devices, the fluid flow is mainly controlled by capillary force and surface tension, while the effect of gravity is less dominant. Capillary rise is not a new phenomenon, but physical experiment can be difficult and costly because the water movement happens very fast and needs accurate equipment. Therefore, this study simulates the capillary rise in micro-tubes using Computational Fluid Dynamics (CFD). The objectives of this study are to observe the transient flow behaviour, compare the effect of different tube radius, and check whether a simplified 2D model can give reasonable result. ANSYS Fluent was used to simulate the two-phase flow between water and air using the Volume of Fluid (VOF) method. The simulation was done using a half-domain 2D model with symmetry boundary, and the mirror feature was only used for clearer contour visualization. A Grid Independence Test (GIT) was carried out to select a suitable mesh. The Continuum Surface Force (CSF) model and laminar viscous model were used to include surface tension effect without adding artificial turbulence. Three tube radius were studied, which were 0.5 mm, 1.0 mm, and 1.5 mm. The results showed underdamped capillary rise oscillation for all cases. The smaller tube had stronger viscous damping and became stable faster. The final capillary heights were 14.75 mm, 7.85 mm, and 6.20 mm for 0.5 mm, 1.0 mm, and 1.5 mm radius, respectively. The result shows that capillary height decreases when tube radius increases, which agrees with the modified Jurin Law for 2D parallel plates. Overall, the 2D VOF model can predict the main capillary rise behaviour with good accuracy.

Keywords:
Capillary rise; surface tension; volume of fluid; micro-tubes; computational fluid dynamics

1. Introduction

Microfluidics is the study of fluid motion at very small length scales (channels, tubes and devices). It is gaining in significance in the modern engineering field, as a large number of systems are being produced in small sizes. They are used in medical diagnostic chips, lab-on-chip devices, inkjet printing, and micro-electronic cooling systems, to name just a few. The liquid needs to flow through extremely

* *Corresponding author.*
E-mail address: iszat@uthm.edu.my

https://doi.org/10.37934/sjotfe.9.1.4959a

small tubes or through small passages in these applications, sometimes without any pump. As a consequence, capillary flow is one of the important flow mechanisms that must be seized properly.

Pressure difference, gravity, and pump power are typically used to control fluid flow in normal large pipes. But if the tube size is very small, then the flow behavior is different. The surface tension force becomes more important compared with the gravity force. Surface tension is the force exerted at the boundary between two fluids, e.g. water and air. If the liquid encounters the wall of a very small tube, the attraction between the liquid and solid wall may be enough to take the liquid up the tube. Capillary rise is the upward flow of water. The final height of the liquid is determined by the surface tension, contact angle, density of the fluid, gravity, and also the radius of the tube.

A long time has passed since the study of capillary rise. Washburn [1] gave one of the earliest equations that describe the flow of liquid in a capillary tube. The washburn equation is useful since it can describe the change in liquid level with time because of capillary force and viscous resistance. Later, Bosanquet [2] added the effect of inertia at the start of the motion to the theory. For low viscosity fluid like water, it is important that the liquid does not rise slowly to the final height. In the initial phase, the water flow can be rapid, it can cross the equilibrium level and then flow back down. This behavior is called underdamped oscillation. With time, the amplitude of oscillation decreases due to damping caused by viscosity at the wall.

Although the capillary rise theory is already well known, it is still not easy to study the full dynamic motion using physical experiment. This can occur quite rapidly, particularly in the initial stages of the rise, especially in the meniscus. For this motion to be seen clearly, high speed camera and accurate measuring equipment is required. Not always an easy task to perform in a student laboratory and it's costly. Therefore, Computational Fluid Dynamics (CFD) is an alternative technique that can be employed to investigate the capillary rise phenomenon. Without undertaking costly experiments, the water-air interface, velocity field and pressure field can be observed in detail using CFD.

The Volume of Fluid (VOF) method is widely used in the simulation of two-phase flows in CFD. A VOF model can be used to follow the interface between the two fluids, air and water, by calculating the volume fraction of each fluid [3]. This is appropriate for a capillary rise simulation as position and shape of the meniscus are significant. The surface tension effect can be captured by incorporating the surface tension force as a source term to the momentum equation, called the Continuum Surface Force (CSF) model [4-8]. The CFD model can be used to simulate the water rising up the micro-tube with the appropriate contact angle and wall adhesion setting.

In several earlier investigations of capillary rise, the actual geometry of the tube was represented by a three-dimensional model. It can produce more realistic shape with 3D model, but more elements are needed and longer simulation time. The student assignment is limited in time and computer capacity of the simulation [9-11]. Thus, if a simplified two-dimensional model can provide reasonable and accurate results, it can be useful. In this study, a 2D planar model is used to reduce computational cost. The model does not intend to completely substitute all 3D simulations; it is used to see if a simplified 2D model can adequately describe the key capillary rise behavior.

Another important parameter in capillary rise is the radius of the tube. Smaller radius of tube should result in a higher capillary rise height (according to Jurin's law). This is because the surface tension force becomes stronger compared with the weight of the liquid column. In a larger radius tube, the mass of the liquid increases and the resultant height of the capillary will decrease [12-16]. Thus, the relationship between geometry size and capillary rise height can be investigated more clearly by comparing the various values of tube radius.

The main aim of this assignment is to simulate capillary rise and surface tension effect in micro-tubes using ANSYS Fluent. Specific aim is to develop a 2D VOF model for the water-air capillary flow, to observe the transient rise and oscillation behavior of the liquid column, to compare the effect of three tube radius which is 0.5 mm, 1.0 mm and 1.5 mm, and to evaluate the accuracy of the CFD results by comparing the obtained with theoretical capillary height. There is also a grid independence test performed to ensure that the result is not significantly dependent on the grid size. This study provides a simple, but clear understanding of the behavior of surface tension-driven flow in micro-tubes.

2. Methodology

This research aims to study the capillary phenomena in micro-tubes using computational fluid dynamics (CFD). The two-phase (water and air) flow is simulated using ANSYS Fluent software. The process is divided into four parts: defining the equations, geometry, mesh, and boundary conditions. The flow is simulated in 2D symmetrical form for computational efficiency but ensuring accurate results for symmetrical circular tubes.

2.1 Geometry Development

A two-dimensional planar domain was used to reduce the computational time. The model consisted of a lower rectangular water reservoir and a vertical micro-tube connected at the centre of the reservoir. Since the geometry was symmetric, only half of the domain was modelled by applying a symmetry boundary at the centreline. Three tube radius were studied, which were 0.5 mm, 1.0 mm, and 1.5 mm. The height of the tube was selected to be higher than the expected capillary rise height so that the liquid column would not reach the top boundary during the simulation. The main dimensions of the computational domain are shown in Figure 1.

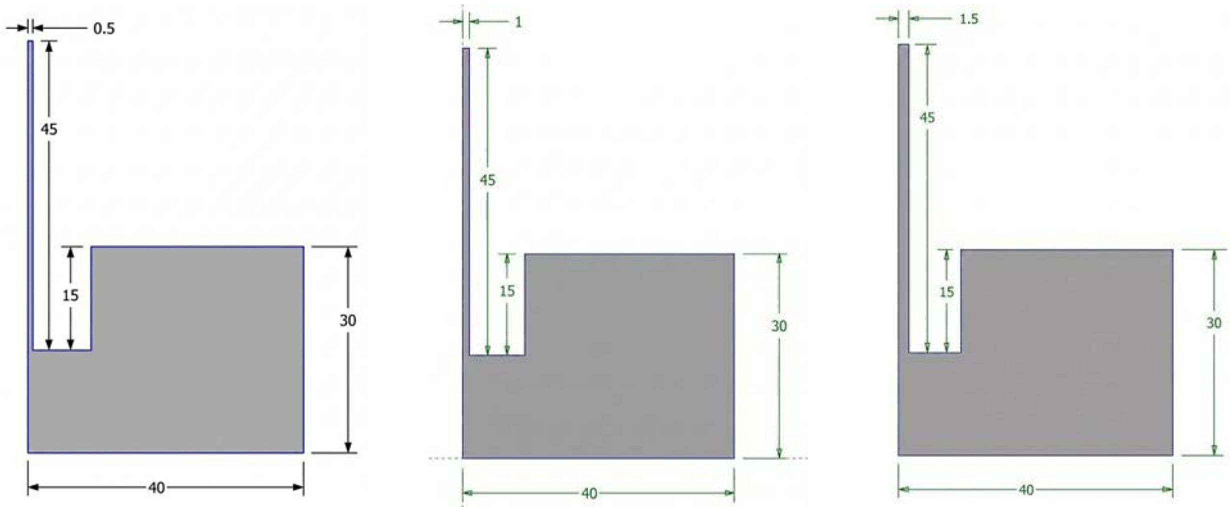

(a) (b) (c)

Fig. 1. Geometry of water tank with micro tube (a) r=0.5 mm (b) r=1 mm (c) r=1.5 mm

2.2 Mesh Generation

The flow domain was meshed by small rectangular structured elements. In capillary flow, it is crucial to have mesh refinement near the wall surface since the contact angle between the water, air and the wall surface is the driving force for the whole capillary flow process [8,17]. So, the mesh was refined near the outer wall of the tube. To make sure that the results don't change with the mesh size, the r=1.0 mm case was run for three different mesh sizes (coarse, medium, fine) in a Grid Independence Test (GIT). A zoomed mesh view near the tube wall was included because the capillary force is highly affected by the interface curvature and wall contact angle. Therefore, a mesh was applied in the tube region and near the tube entrance to reduce numerical error.

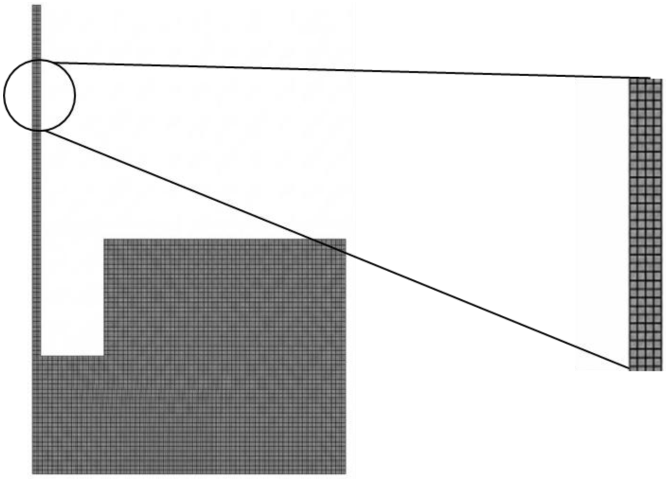

Fig. 2. Computational mesh of the capillary rise domain

2.3 Grid Independence Test Procedure

A Grid Independence Test (GIT) was carried out to check whether the CFD result was affected by the mesh size. This step is relevant because the very coarse mesh may lead to an incorrect capillary height and the very fine mesh will make the calculation be more time consuming. The middle size of the three tested geometries was chosen to be r = 1.0 mm micro-tube and used in the GIT for this study. Three meshes – coarse, medium and fine – were prepared. The geometry, material properties, boundary conditions, the surface tension value, contact angle, time step and solver settings were the same for each mesh case. Only the mesh size was varied. This is to ensure that the difference in the result is only due to the number of meshes, and not due to any other setting.

Capillary height at final equilibrium was chosen as the primary parameter to be compared. The selected parameter was chosen since the main object of the simulation is to predict the height of the capillary rise inside the micro-tube. Once all three mesh cases were finished, the final capillary height for each mesh was compared. However, if the difference between the medium and fine mesh is small, the sensitivity to mesh size can be regarded as less. The mesh which provides acceptable accuracy and lower computational cost was then chosen to use in the other simulations.

The result of the GIT is reported and will be discussed in Results section. This separation is carried out to explain how the test was performed in the Methodology section and to present the values obtained as well as the selected mesh in the Results section.

2.4 Boundary Condition and Solver Settings

The simulation was run as Transient because capillary rise is an unsteady process where the water level rises and oscillates. The gravity was turned on and set to -9.81 ms^{-2} in the Y-axis. The Volume of Fluid (VOF) model was selected, where air was the primary phase and liquid water the secondary phase. To allow the simulation to run, the patch initialization function was applied to fill the bottom tank with water (volume fraction of water = 1) and the vertical micro-tube with air. The outlet of the volume was defined as a pressure outlet at the atmospheric pressure. The wall boundaries had the

"Wall Adhesion" option enabled to model the surface tension effect. The static contact angle for the micro-tube was set to 0° (perfectly wetting surface) and 90° for the tank wall.

The "Implicit Body Force" option was turned on to enhance the calculation stability and minimize spurious velocities. To ensure good convergence for multiphase flows, the Coupled scheme was used for pressure-velocity coupling. For numerical schemes, the pressure was interpolated using the PRESTO! scheme and the volume fraction used the Compressive scheme to maintain a very sharp water-air interface. To calculate the momentum, the Second Order Upwind scheme was selected, and the temporal transient scheme was set to First Order Implicit. A very small-time step was used to capture the underdamped vibration of the water level. Additionally, in ANSYS Fluent, a surface monitor was created to track the maximum Y-coordinate (height) of water at each time step; the transient data was then exported to Microsoft Excel to generate a plot. The solver settings are listed in Table 1

Table 1
Summary of the solver setup and boundary conditions

Parameter	Setting
Multiphase model	Volume of fluid (VOF), implicit body force
Phase definition	Primary phase: Air, secondary phase: Water-liquid
Gravity	Y = -9.81 ms^{-2}
Surface tension	0.072 N/m (continuum surface force model)
Wall adhesion (contact angle)	Tube wall = 0°, tank wall = 90°
Initialization method	Patch 1 (Tank) = Water, patch 2 (tube) = air
Pressure-velocity coupling	Coupled scheme
Spatial discretization (pressure)	PRESTO!
Spatial discretization (volume fraction)	Compressive
Transient formulation	First order implicit

2.5 Governing Equations

The flow is simulated by solving the basic conservation equations for mass and momentum. Because we are calculating the flow of two fluids, water and air, that do not mix, the Volume of Fluid (VOF) method is used to calculate the location of the interface [3,18-20]. The continuity equation for the volume fraction of the second phase (water-liquid <l>), a_q is solved to determine the water's location.

$$\frac{\partial a_g}{\partial t} + \nabla.\left(a_q v\right) = 0 \tag{1}$$

The momentum equation was shared between the phases. The surface tension force is added as a source term in the momentum equation using the Continuum Surface Force (CSF) model proposed by Brackbill *et al.,* [4]. This is the most important force that drives the water up the micro-tube.

$$\frac{\partial}{\partial t}(pv) + \nabla.(pvv) = -\nabla p + .[\mu(\nabla v + \nabla v^{t})] + pg + F_{CSF} \tag{2}$$

2.6 Post-Processing and Analysis

Once the transient calculation was performed, the analysis of the results was carried out with the post processing tools of ANSYS Fluent. Major results that were extracted from Fluent were water volume fraction contour, static pressure contour, velocity contour, and transient capillary height data. The results were used to investigate the capillary rise phenomena within the micro-tube and the capillary rise effect of the different tube radius.

The geometry was symmetric along the centreline of the tank and the micro-tube and hence the simulation was carried out only for half of the tank and micro-tube. The simulation was carried out with the centreline as a symmetry boundary condition. Once the calculation is complete, only the mirror display feature of ANSYS Fluent is used to visualize the calculation result. This means that the numerical value didn't change or improve by using the mirror feature. It did little to reveal the contour as a whole tank/tube shape so that the interface between water and air, pressure distribution, and the velocity field would be seen more clearly.

The water volume fraction contour was used to determine water and air regions. The volume fractions in the water and air regions were nearly 1 and 0, respectively. The meniscus shape and the final height of the capillary were observed at the interface of these two phases. To explain the pressure distribution within the tank and tube, the pressure contour was used and to observe the flow motion during and after the capillary rise process, the velocity contour was used. The transient capillary height data was captured in the simulation and exported to Microsoft Excel. The graph of capillary height vs. flow time was then plotted to analyze the initial rise, overshoot, oscillation, dampening, and final capillary height equilibrium of the water column. All the contours were post-processed in a similar manner, as much as possible, to make the comparison between different tube radius clearer and fair.

3. Results

In this chapter, the capillary rise behaviour in micro-tubes was analysed using ANSYS Fluent. The results include the transient capillary height, pressure contour, velocity contour, and water volume fraction contour. Three tube radii were compared, which were 0.5 mm, 1.0 mm, and 1.5 mm. The numerical results were also compared with the theoretical capillary height to evaluate the accuracy of the CFD model.

3.1 Grid Independence Test

To validate the accuracy of the simulation results and to ensure that they are not influenced by the mesh density, a grid independence test (GIT) was conducted on the r = 1.0 mm micro-tube. We established three types of meshes: coarse (GIT 1), medium (GIT 2) and fine (GIT 3). The height of the capillary equilibrium was compared for each case under the same boundary conditions, as listed in Table 2. The final capillary height changed from 7.50 mm for the coarse mesh to 7.85 mm for the medium mesh. When the mesh was further refined to the fine mesh, the height changed to 7.59 mm.

Table 2
Parameters and results for the grid independency test

Parameter	GIT 1 Coarse	GIT 2 Medium	GIT 3 Fine
Element size (mm)	0.5	0.25	0.1
Number of nodes	9221	18161	112001
Number of elements	8880	17700	110850
Final capillary height (mm)	7.5	7.85	7.59

The percentage difference between the medium and fine mesh was about 3.3%, which is considered acceptable for this assignment. Therefore, the medium mesh was selected for the remaining simulations because it provided reasonable accuracy with lower computational cost.

However, the result was not fully monotonic, so the mesh independence result should be interpreted as an acceptable engineering approximation rather than a perfectly converged solution.

3.2 Transient Dynamics and Oscillatory Behaviour

The millimeter-scale tubes of low-viscosity fluids like water, capillary rise is essentially a dynamic and time-dependent phenomenon. To explore this in detail the transient behaviour was measured in all geometries. Figure 3 shows the capillary height and flow time of the three tube radii (r = 0.5 mm, 1.0 mm and 1.5 mm). In all the cases, the driving surface tension force at first accelerates the water upward with high velocity as shown in Figure 3. Because of inertia of the fluid, the columns of water initially over-shoot their eventual equilibrium points, and then the force of gravity and friction of the walls slow down the movement. The graphs already prove the fact that the tube radius does influence considerably the final height of the oscillation as well as the damping ratio of the oscillation.

With the smallest tube (r = 0.5 mm), the fluid reached the highest initial peak (about 41 mm) and settled in the highest equilibrium point of about 14.71 mm. It is interesting to note that its oscillation decayed very fast reaching the highest equilibrium point within less than 1.0 seconds. It happens since under a small diameter of the tube the viscous friction of the wall is extremely dominant in comparison with the mass of the fluid and quickly exhausts the kinetic energy. On the other hand, the equilibrium heights dropped to about 7.34 mm and 5.9 mm as the radius was changed to 1.0 mm and 1.5 mm, respectively.

Moreover, the biggest tube (r = 1.5 mm) showed a very underdamped behaviour evolving indefinitely after 3.0 seconds. This is since the greater the mass of the fluid, the greater the inertial force is and the lesser the relative impact of the wall friction and therefore, the kinetic energy enables the oscillatory "bouncing" to be extended within a substantially longer duration. This fidelity of the inertial and viscous damping effects is an indication of the high fidelity of the adopted transient CFD methodology.

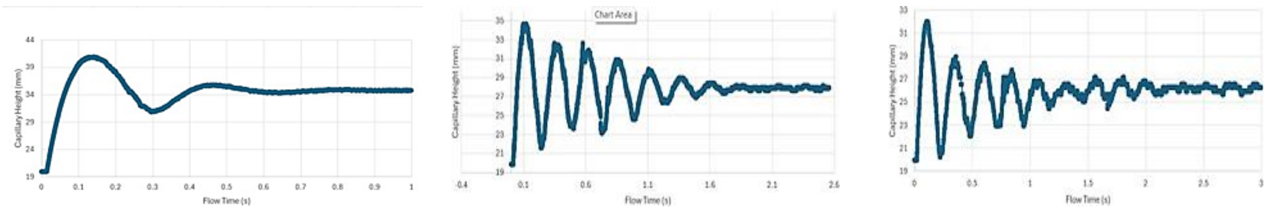

(a) (b) (c)

Fig. 3. Comparison of transient capillary height and underdamped oscillation across different tube radius (a) r=0.5 mm (b) r=1 mm (c) r=1.5 mm

3.3 Flow Dynamics: Pressure and Velocity Characteristics

The visualisations of the static pressure profile and velocity profile were then obtained at the three tube radii when the capillary flow was in its ultimate steady-state equilibrium such as the water level was held constant. Figures 4 and 5 shown the static pressure and velocity plots of the 0.5 mm, 1.0 mm and 1.5 mm geometries. The hydrostatic pressure gradient and the mechanism of capillary action can be well visualized using the contours of the static pressure. As it would be expected, the pressure is greatest at the bottom of the reservoir (as shown by the red area) and it declines gradually with height. Above all, there is a clear Laplace pressure difference at the air-water interface within the micro-tubes. The pressure on the concave air side is slightly greater than the pressure on the convex water side forming the maintained suction force required to counter the weight of the liquid column.

The velocity contours on the other hand illustrate the flow behaviour once the initial dynamic oscillations had died off. Since the fluid has settled to the maximum height, and the macroscopic upward movement is no longer possible, the velocity within the bulk of the micro-tubes is mainly zero (shown by the solid blue areas). Nevertheless, there are localized areas of small magnitude of velocity (which can be seen as green/red areas) around the entrance of the micro-tubes and the bottom of the reservoir. These are common residual micro-vortices due to dissipation of energy as the bulk fluid slows down to a complete halt. The residual velocity disturbances are found to be less in the narrower tube (0.5 mm) than in the wider tubes, which also supports the conclusion that smaller geometries undergo greater viscous damping effects.

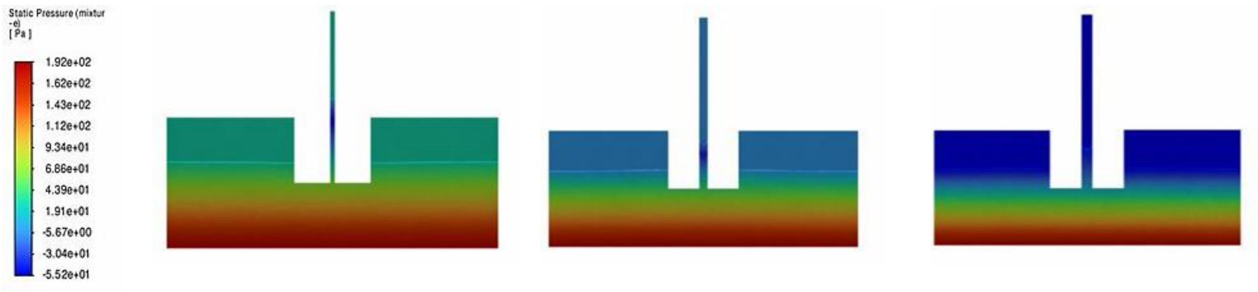

(a) (b) (c)

Fig. 4. Static pressure contour (a) 0.5 mm (b) 1.0 mm (c) 1.5 mm

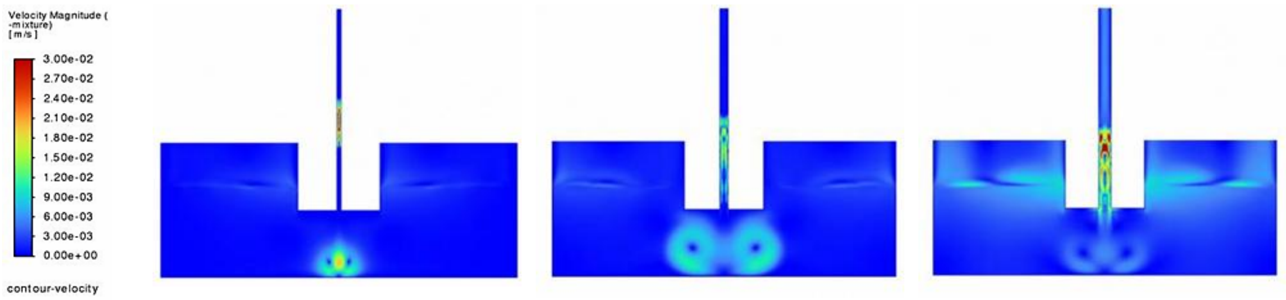

(a) (b) (c)

Fig. 5. Velocity contour (a) 0.5 mm (b) 1.0 mm (c) 1.5 mm

3.4 Comparative Study: Effect of Tube Radius

To satisfy the assignment's extension requirement, a comparative study was conducted on three different tube geometries. Figure 6 shows the steady-state phase contours (water volume fraction) for tube radius of 0.5 mm, 1.0 mm, and 1.5 mm. The simulations demonstrate a clear inverse relationship between the tube radius and the equilibrium height, which strongly agrees with Jurin's Law. The smallest geometry (r = 0.5 mm) generated the highest capillary rise at 14.75 mm. When the radius was doubled to 1.0 mm, the height significantly dropped to 7.85 mm. Finally, the largest tube (r = 1.5 mm) recorded the lowest equilibrium height at 6.20 mm. The contours also show that the meniscus curvature was perfectly preserved across all scales.

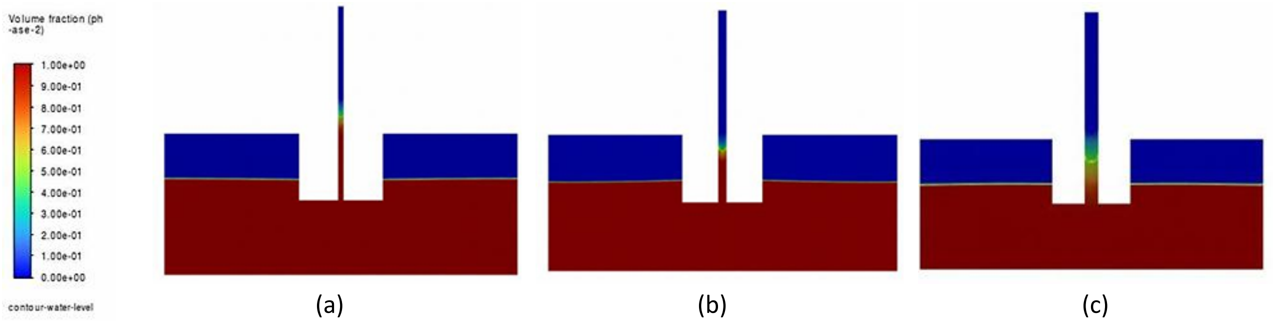

Fig. 6. Steady-state phase contours (a) r = 0.5 mm (b) r = 1.0 mm (c) r = 1.5 mm

3.5 Discussion and Accuracy Analysis

The accuracy of the CFD results was also critically evaluated by comparing the CFD equilibrium heights with the theoretical (classical) values. The impact of the selected parameters of the CFD domain should be mentioned. Since it used a 2D planar space to simulate, the model can be seen as a physical model of the capillary rise between two infinite parallel plates with a half-width of r, and not a 3D cylindrical tube. This 2D planar configuration has a modified equation that controls the theoretical capillary height,

$$h = \frac{\gamma cos\theta}{pgr} \tag{3}$$

Using the standard properties of water (γ= 0.072Nm−1, ρ= 998.2kgm−3), the theoretical height for the 0.5 mm model is calculated to be 14.71 mm. The CFD simulation recorded a final height of 14.75 mm, resulting in an exceptionally low error margin of less than 0.3%. This remarkable accuracy validates the chosen multiphase CFD parameters.

Various important numerical techniques helped to achieve this accuracy. First, the mesh refinement was concentrated around the wall to make sure that the static contact angle (0°) was solved exactly, the upward surface tension force was computed without spatial discretization errors. Secondly, an interpolation of the pressure by the PRESTO! scheme, together with Compressive volume fraction scheme, was used to avoid the flattening of the air-water interface, leaving the meniscus very sharp. The turn on of the "Implicit Body Force" formulation also played an essential role in eliminating spurious velocity currents which usually destabilize multiphase VOF models.

Finally, in the turbulence model, a viscous model (Laminar) was selected intentionally as opposed to a turbulent model (e.g., k-ε or k-ω SST). Since micro-channel capillary flows are at very low Reynolds numbers, the addition of a turbulence model would physically wrongly model the flow and would artificially add turbulent viscosity that would falsely damp the oscillatory behaviour that was found in Section 3.1. In general, the chosen 2D laminar-VOF approach was very robust and precise to this internal flow phenomenon.

4. Conclusions

In this study, it was successfully simulated the capillary rise and surface tension effect in the micro-tubes by using a 2D VOF model in ANSYS Fluent. The main aim of this assignment was accomplished as the program was able to display the transient rise of the water in the micro-tube, the underdamped oscillation behaviour and the final equilibrium height of the water inside the micro-tube.

The grid independence test showed that the mesh size can affect the final capillary height. Based on the comparison of the three mesh sizes (coarse, medium and fine), the medium mesh size was chosen in the further simulations due to the acceptable accuracy yet lower computation cost. This ensured that the latter results were not unduly influenced by an inappropriate mesh.

From the transient results, it could be seen that the water level increased rapidly at the initial stage, which was caused by the surface tension force. Then the water column reached a height above the target, using oscillations before coming to a stable state. The reason for this behaviour was a balance between surface tension, inertia, gravity and viscous damping. The pressure contour also indicated the pressure gap that provided the capillary action, and the velocity contour indicated that the flow was very low after it reached steady state.

It was revealed that the tube radius has a definite effect on the capillary rise height when comparing the three different tube radius. The lowest radius of 0.5 mm, gave the maximum final capillary height of 14.75 mm. The 1.0 mm radius resulted in a final height of 7.85 mm and the 1.5 mm radius resulted in the lowest final height of 6.20 mm. This indicates that the smaller the radius of the tube, the greater is the capillary rise, which agrees with the theoretical prediction.

Overall, the 2D VOF model was able to predict the main behaviour of capillary rise in micro-tubes with good accuracy. It was also shown that a simplified 2D simulation can be a valuable tool when the goal is to understand the overall trend and to compare the effect of the various tube radius, in the present case the problem of a surface tension driven flow.

References

[1] Washburn, Edward W. "The dynamics of capillary flow." *Physical review* 17, no. 3 (1921): 273. https://doi.org/10.1103/PhysRev.17.273

[2] Bosanquet, C. H. "LV. On the flow of liquids into capillary tubes." *The London, Edinburgh, and Dublin Philosophical Magazine and Journal of Science* 45, no. 267 (1923): 525-531. https://doi.org/10.1080/14786442308634144

[3] Hirt, Cyril W., and Billy D. Nichols. "Volume of fluid (VOF) method for the dynamics of free boundaries." *Journal of Computational Physics* 39, no. 1 (1981): 201-225. https://doi.org/10.1016/0021-9991(81)90145-5

[4] Brackbill, Jeremiah U., Douglas B. Kothe, and Charles Zemach. "A continuum method for modeling surface tension." *Journal of Computational Physics* 100, no. 2 (1992): 335-354. https://doi.org/10.1016/0021-9991(92)90240-Y

[5] Ubbink, Onno, and RI1703648 Issa. "A method for capturing sharp fluid interfaces on arbitrary meshes." *Journal of Computational Physics* 153, no. 1 (1999): 26-50. https://doi.org/10.1006/jcph.1999.6276

[6] Oefelin, Joseph, and Vigor Yang. "Analysis of transcritical spray phenomena in turbulent mixing layers." In *34th Aerospace Sciences Meeting and Exhibit*, p. 85. 1996. https://doi.org/10.2514/6.1996-85

[7] Afkhami, Shahriar, Stephane Zaleski, and Markus Bussmann. "A mesh-dependent model for applying dynamic contact angles to VOF simulations." *Journal of computational physics* 228, no. 15 (2009): 5370-5389. https://doi.org/10.1016/j.jcp.2009.04.027

[8] Popinet, Stéphane. "An accurate adaptive solver for surface-tension-driven interfacial flows." *Journal of Computational Physics* 228, no. 16 (2009): 5838-5866. https://doi.org/10.1016/j.jcp.2009.04.042

[9] Tehrani, Ramin Mohamed Ali, and Sulaiman Ab Ghani. "The hexagonal close-packed nickel nanocrystals prepared by fast scan voltammetry." *Journal of colloid and interface science* 339, no. 1 (2009): 125-132. https://doi.org/10.1016/j.jcis.2009.07.042

[10] Kishor, D. Krishna, S. Gopalakrishnan, and Ranjan Ganguli. "A Legendre spectral element model for sloshing and acoustic analysis in nearly incompressible fluids." *Journal of Computational Physics* 229, no. 7 (2010): 2605-2624. https://doi.org/10.1016/j.jcp.2009.12.008

[11] Stange, Michael, Michael E. Dreyer, and Hans J. Rath. "Capillary driven flow in circular cylindrical tubes." *Physics of fluids* 15, no. 9 (2003): 2587-2601. https://doi.org/10.1063/1.1596913

[12] Fries, N., and M. Dreyer. "The transition from inertial to viscous flow in capillary rise." *Journal of colloid and interface science* 327, no. 1 (2008): 125-128. https://doi.org/10.1016/j.jcis.2008.08.018

[13] Kazemzadeh, Amin, Poo Ganesan, Fatimah Ibrahim, Shuisheng He, and Marc J. Madou. "The effect of contact angles and capillary dimensions on the burst frequency of super hydrophilic and hydrophilic centrifugal microfluidic platforms, a CFD study." *PloS one* 8, no. 9 (2013): e73002. https://doi.org/10.1371/journal.pone.0073002

[14] Das, Siddhartha, and Sushanta K. Mitra. "Different regimes in vertical capillary filling." *Physical Review E* 87, no. 6 (2013): 063005. https://doi.org/10.1103/PhysRevE.87.063005

[15] Wörner, Martin. "Numerical modeling of multiphase flows in microfluidics and micro process engineering: a review of methods and applications." *Microfluidics and Nanofluidics* 12, no. 6 (2012): 841-886. https://doi.org/10.1007/s10404-012-0940-8

[16] Raeini, Ali Q., Martin J. Blunt, and Branko Bijeljic. "Modelling two-phase flow in porous media at the pore scale using the volume-of-fluid method." *Journal of Computational Physics* 231, no. 17 (2012): 5653-5668. https://doi.org/10.1016/j.jcp.2012.04.011

[17] Yan, Wenli, Guimei Lin, Rong Zhang, Zhen Liang, Lixian Wu, and Wenjuan Wu. "Studies on molecular mechanism between ACE and inhibitory peptides in different bioactivities by 3D-QSAR and MD simulations." *Journal of Molecular Liquids* 304 (2020): 112702. https://doi.org/10.1016/j.molliq.2020.112702

[18] Vachaparambil, Kurian J., and Kristian Etienne Einarsrud. "Comparison of surface tension models for the volume of fluid method." *Processes* 7, no. 8 (2019): 542. https://doi.org/10.3390/pr7080542

[19] Popescu, Mihail Nicolae, John Ralston, and Rossen Sedev. "Capillary rise with velocity-dependent dynamic contact angle." *Langmuir* 24, no. 21 (2008): 12710-12716. https://doi.org/10.1021/la801753t

[20] Khanjani, Elham, Andrea Fergola, Joan Antoni López Martínez, Simin Nazarnezhad, Jasmina Casals Terre, Simone Luigi Marasso, and Behrouz Aghajanloo. "Capillary microfluidics for diagnostic applications: fundamentals, mechanisms, and capillarics." *Frontiers in Lab on a Chip Technologies* 4 (2025): 1502127. https://doi.org/10.3389/frlct.2025.1502127